Eur. J. Mineral.
2001, **13**, 769–777

Ekatite, $(Fe^{3+},Fe^{2+},Zn)_{12}(OH)_6[AsO_3]_6[AsO_3,HOSiO_3]_2$, a new mineral from Tsumeb, Namibia, and its crystal structure

PAUL KELLER

Institut für Mineralogie und Kristallchemie, Universität Stuttgart, Pfaffenwaldring 55,
D-70569 Stuttgart, Germany. – e-mail: paul.keller@po.uni-stuttgart.de

Abstract: Ekatite, ideally $(Fe^{3+},Fe^{2+},Zn)_{12}(OH)_6[AsO_3]_6[AsO_3,HOSiO_3]_2$, is a new mineral from Tsumeb, Namibia. It is associated with chalcocite and occurs as small sprays of fine needles, up to 2 mm long and less than 0.2 mm in diameter. Ekatite is brownish black, translucent with a brown streak and vitreous lustre. It is brittle without cleavage and its Mohs' hardness is ~3. The mineral is non-fluorescent, optically uniaxial positive with indices of refraction ω ~1.99 and ε ~2.08, pleochroic with ω = dark brownish black and ε = medium brown. Microprobe analysis revealed the following chemical composition (in wt%): (total Fe given as) Fe_2O_3 50.79, ZnO 3.78, As_2O_3 42.50, and SiO_2 2.10. The empirical formula based on 20 cations and the results of structure determination is: $(Fe^{3+}_{5.95}Fe^{2+}_{5.14}Zn_{0.81})_{\Sigma 11.90}(OH)_{6.00}(As_{1.01}O_3)_{6.00}[(AsO_3)_{1.43}(HOSiO_3)_{0.61}]_{\Sigma 2.04}$. Single crystal X-ray studies give the following parameters: hexagonal, space group $P6_3mc$; $a = 12.773(2)$, $c = 5.051(1)$ Å, $V = 713.7(4)$ Å^3 with $Z = 1$; $D_{calc} = 4.061$ g/cm^3. The strongest reflections of the powder pattern are [d_{obs} in Å, (I_{vis}) and (hkl_{hex})]: 11.11 (3) (100), 6.37 (5) (110), 3.220 (10) (211, 220), 2.766 (3) (400), 2.420 (7) (401, 410), 1.867 (3) (402), 1.672 (3) (521), and 1.508 (3) (701, 531). The crystal structure was solved by direct methods and refined to R = 0.043 using 980 observed unique reflections. It contains dimers of face-sharing $(Fe^{3+},Fe^{2+},Zn)O_4(OH)_2$ octahedra, which are linked together by common edges to form infinite double chains. They are connected by corners to form a three-dimensional framework with two types of channels running along the *c*-axis. The larger is hexagonal and lined by six AsO_3-groups, in such a way that the lone-pairs of As^{3+} point to its centre. Trigonal pyramids of AsO_3 and $HOSiO_3$ tetrahedra, in random distribution, occupy the smaller triangular channel, with either the lone pairs or the OH oriented along the *c*-axis. Ekatite is structurally related to phosphoellenbergerite, ellenbergerite and holtedahlite, as well as to several transition-metal tellurites, selenites, phosphites and $Zn_7(OH)_3(SO_4)(VO_4)_3$.

The name is in honour of Dieter Ekat (1935-1996), a Namibian mining engineer.

Key-words: ekatite, new mineral, crystal structure, Fe arsenite/silicate, Tsumeb, Namibia.

Introduction

The new mineral species was brought to our attention by Michael Grieser, Mannheim, who submitted it for identification. During the course of description, Herbert Nägele, Windhoek, donated a second specimen with the new mineral.

The new mineral name honours Dieter Ekat (1935-1996), a mining engineer and former owner of the Rubicon mine, Namibia. Both name and species have been approved by the Commission on New Minerals and Mineral Names (CNMMN) of IMA as No. 98-024. The type material is deposited at the Museum of the Institut für Mineralogie und Kristallchemie, Universität Stuttgart, catalogue No. NM20. Keller *et al.* (1999) have presented some structural details of the species fully described here.

Occurrence

Ekatite is a new species from Tsumeb, Namibia, that can be added to the long list of type minerals from this exceptional locality (Keller, 1984; Geb-

0935-1221/01/0013-0769 $ 2.25

DOI: 10.1127/0935-1221/2001/0013-0769

Fig. 1. Ekatite forming a small spray of fine needles on a matrix of corroded quartz.

hard, 1991). The secondary mineral was found on a matrix of etched quartz and chalcocite. Unfortunately, there is no exact information about the sampling location in the mine. Both specimens have been acquired from the same dealer in Tsumeb. According to him, they were collected at "deep levels". This fits well with the occurrence of other As^{3+}-bearing minerals from the "second oxidation zone" like leiteite, $Zn(As^{3+}{}_2O_4)$, schneiderhöhnite, $Fe^{2+}Fe^{3+}{}_3(As^{3+}O_3)(As^{3+}{}_2O_5)_2$, ludlockite, $PbFe^{3+}{}_4(As^{3+}{}_5O_{11})_2$, claudetite, As_2O_3, arsenolite, As_2O_3, *etc.* (Keller, 1984; Keller & Innes, 1986).

Physical properties

Ekatite forms small sprays of striated, fine needles. They are elongated along the *c*-axis, up to 2 mm long but less than 0.2 mm in diameter (Fig. 1). There are indistinct (hk0) forms, but no termination could be detected. The mineral is brittle without distinct cleavage. The Mohs' hardness is about 3. Ekatite is brownish black, with a brown streak, translucent and displays bright vitreous lustre. It is optically uniaxial positive with indices of refraction $\omega \sim 1.99$ and $\varepsilon \sim 2.08$. According to the Gladstone-Dale relationship (Mandarino, 1981), the compatibility index $1-(K_p/K_c) = 0.007$ is superior for the mean measured and the calculated index of refraction $n_{meas.} \sim 2.02$ and $n_{calc.} = 2.013$, respectively. The mineral is non-fluorescent, strongly pleochroic with ω = dark brownish black and ε = medium brown, both with a greenish tint. Although the colours are not typical, Fe^{3+}-Fe^{2+} charge transfer between face-sharing octahedra may account for the pleochroism.

Chemistry

Ekatite was initially analysed using a Microspec WDX-400 wavelength-dispersive system of a Scamscan CS44 with an operating voltage of 30 kV and a beam current of 20 nA (Table 1). The following standards were used for calibration: SiO_2 (Si), FeS_2 (Fe), Zn (Zn) and GaAs (As). To verify the small amount of SiO_2, independent analyses were carried out with a Cameca Camebax SX50 electron microprobe (University Paul Sabatier, Toulouse, France) operated at 15 kV and 20 nA (for all elements), and the standards wollastonite (Si), Fe_2O_3 (Fe), ZnS (Zn) and As (As) (Table 1). The presence of OH has been proved by IR-spectroscopy, which shows two absorption bands with wavenumbers

Table 1. Chemical composition of ekatite.

	Scam scan Stuttgart	Atomic proport.1)	Cameca Toulouse	Atomic proport.1)	Mean wt%	Atomic prop.1)	Required compos.	Ideal. compos.
$Fe_2O_3$2)	27.41	5.93	27.11	5.96	27.26	5.95	27.17	27.45
FeO2)	21.18	5.09	21.20	5.18	21.19	5.14	21.12	21.41
ZnO	3.94	0.84	3.66	0.79	3.80	0.81	3.79	3.73
As_2O_3	42.95	7.50	42.16	7.48	42.56	7.49	42.41	41.94
SiO_2	2.21	0.63	2.02	0.59	2.12	0.61	2.11	2.07
H_2O3)	3.46	6.64	3.38	6.59	3.42	6.61	3.41	3.40
Sum	101.15		99.53		100.35		100.00	100.00

1): On the basis of 20 cations; 2): Fe^{3+} and Fe^{2+} calculated on the basis of the structure determination; 3): from OH(4) and OH(5) according to the structure determination

Table 2. X-ray powder diffraction data for ekatite.

hkl	$d_{calc.}$	$d_{obs.}$	$I_{calc.}$	$I_{vis.}$
100	11.062	11.11	56	30
110	6.386	6.37	11	50
200	5.531	5.52	6	10
101	4.595	4.60	30	20
210	4.181	4.18	3	10
201	3.730	3.69	3	20
301	3.687		9	
211	3.221	3.220	100	100
220	3.193		16	
310	3.068	3.070	1	5
301	2.978	2.975	10	10
400	2.765	2.766	23	30
311	2.622	2.620	9	10
320	2.538	2.531	5	20
002	2.526		5	
401	2.426	2.420	29	70
410	2.414		8	
112	2.349	2.349	7	10
202	2.297	2.300	14	10
321	2.267	2.262	5	10
500	2.212	2.210	4	10
411	2.178	2.179	5	5
501	2.027	2.028	7	10
222	1.981	1.982	18	10
421	1.932	1.931	4	20
402	1.865	1.867	3	30
511	1.849	1.849	6	20
430	1.819	1.815	3	5
322	1.790	1.788	7	20
520	1.771	1.771	1	10
412	1.745	1.746	1	10
431	1.711	–	10	–
610	1.687	1.689	2	10
521	1.672	1.672	10	30
440	1.595	1.595	8	20
530,700	1.580	1.582	3	10
521,213	1.562	1.561	1	10
701,531	1.508	1.507	3	30

Indexing and $d_{calc.}$ based on the unit cell dimensions *a* 12.773, and *c* 5.051 Å obtained from single crystal study. $d_{obs.}$ determined with a Debye-Scherrer camera, 57.3 mm, and Mn-filtered Fe-Kα radiation. The relative intensities $I_{vis.}$ and $I_{calc.}$ are visually estimated and calculated from the crystal structure, respectively.

3484 and 3465 cm^{-1}. No other elements than those mentioned above have been detected. The oxidation states of As and Fe, as well as H_2O content are given according to stoichiometry and the results of structure determination, as described below. The empirical formula of ekatite based on 20 cations is $(Fe^{3+}{}_{5.95}Fe^{2+}{}_{5.14}Zn_{0.81})_{\Sigma 11.90}(OH)_{6.00}(As_{1.01}O_3)_{6.00}$ $[(AsO_3)_{1.43}\,(HOSiO_3)_{0.61}]_{\Sigma 2.04}$ (Table 1).

X-ray crystallography and structure determination

An indexed powder diffraction pattern is given in Table 2. It was obtained with a 57.3 mm Debye-Scherrer camera and Fe*K*α radiation, filtered with Mn. No internal standard was used. The relative intensities are visually estimated. For comparison, the powder pattern calculated on the basis of structure determination is added.

A fragment of a single crystal, showing (hk0) faces, was measured on a Stoe IPDS equipment with monochromatized Mo*K*α radiation. Two hundred images with Δϕ 1° were exposed at a duration of 3 minutes each. The image plate was set to 60 mm, which resulted in a maximum of 2Θ 66°. The absorption was corrected using the HABITUS program (Herrendorf, 1997) for 671 equivalents and 81 unique reflections. Transmission factors ranged between 0.5621 and 0.8251. All other essential measuring parameters are given in Table 3.

Systematic absences and reflection statistics indicate the non-centrosymmetric space groups $P6_3$ and $P6_3mc$ without any systematic absence violations. Since $P6_3$ is a subgroup of $P6_3mc$, the latter was initially used for structure determination by direct methods with the SHELXTL program package (SHELXTL, 1996). It yielded the position of M(1) ≡ Fe^{3+}, As(1), As(2), O(1) to O(3) and OH(4). Structure refinement on F^2 with the SHELXL97 program (SHELXL-97, 1997) was performed in several steps. The position M(1) on (12d) was refined for Fe^{3+}, Fe^{2+} and Zn by applying constraints and restraints of the SHELXL97 program: the same atomic coordinates were used for all three atoms by the constraint EXYZ and the same displacement parameters by the constraint EADP; SUMP restraints were applied to fix the average charge to 2.5 and the sum of occupancy to 1.0. The results are in relatively good agreement with the chemical analyses (Tables 1 and 4). In a second refinement step the position of As(2) was split by introducing Si(2). Both could be refined anisotropically without any constraint or restraint. Then OH(5) was introduced by selecting a peak from the difference-Fourier map. It was isotropically refined with fixed occupancy according to the result of chemical analyses. Finally, two H were added with coordinates from the difference-Fourier map. They could be re-

Table 3. Experimental details and crystallographic data for ekatite.

Crystal data	
Space group	$P6_3mc$
a [Å]	12.773(2)
c [Å]	5.051(1)
V [Å^3]	713.7(4)
Z	1
$D_{calc.}$ [g/cm^3]	4.061
μ [mm^{-1}]	14.82
Size [mm]	0.3, 0.15, 0.1
Intensity measurements	
Diffractometer	Stoe IPDS
Monochromator	graphite
Radiation	Mo-$K\alpha$
$2\Theta_{max}$ [°]	65.65
$h_{min.}$, $h_{max.}$	-18, 19
$k_{min.}$, $k_{max.}$	-19, 19
$l_{min.}$, $l_{max.}$	-7, 7
Observed reflections	10026
Unique reflections	982
R_{inter}	0.069
R_σ	0.026
Temperature [°C]	25
F(000)	819.2
Structure determination and refinement	
Reflections used	980
Reflections with $F_o>4\sigma(F_o)$	938
Parameters refined	65
Extinction	0.0064
$R_1(F)\{F_o>4\sigma(F_o)\}$	0.043
R_1(all)	0.046
wR_2(all)	0.116
Weighting parameters	0.0265
	13.27
GooF	1.268
Flack-x-parameter	0.0108
(Δρ)max [e/A^3]	2.58
(Δρ)min [e/A^3]	-1.49
Rms [e/A^3]	0.33

fined isotropically, but only with fixed occupancy parameters. More details of the structure determination and refinement are given in Table 3. The final atomic coordinates and equivalent displacement parameters are given in Table 4.

Structure determination and refinement were also performed in the subgroup $P6_3$, mainly to check the ordering of the di- and tri-valent cations. The final R-values for $P6_3$, however, are slightly worse than those obtained for space group $P6_3mc$ (Table 3): $R_1(F)\{F_0>4\sigma(F_0)\}$ 0.045; R_1(all) 0.049; wR_2(all) 0.1136; GooF 1.315.

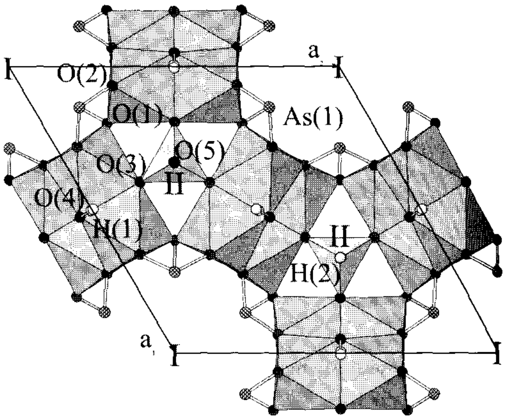

Fig. 2. Crystal structure of ekatite projected onto the (001) plane. The polyhedra represent the octahedra of $M(1)O_4(OH)_2$ and the tetrahedra of $HOSi(2)O_3$, which envelop the $As(2)O_3$ groups. The hexagonal and triangular channels are indicated with I and II, respectively.

Description and discussion of the crystal structure

The most impressive features of the ekatite framework structure are (i) densely packed trigonal rods centred on the three-fold axes, consisting of $M(1)O_4(OH)_2$, $As(2)O_3$ and $HOSi(2)O_3$ groups, as well as (ii) large hexagonal channels along the 6_3 screw axes that contain only $As(1)O_3$ groups (Fig. 2, 5a). Ekatite represents a new mineral structure type. Some interesting structural relations to few other minerals, especially phosphoellenbergerite, $P6_3mc$ (Brunet & Schaller, 1996; Raade *et al.*, 1998), ellenbergerite, $P6_3$ (Chopin *et al.*, 1986; Comodi & Zanazzi, 1993), holtedahlite, $P31m$ (Rømming & Raade, 1989) and a number of chemical compounds, will be discussed in the last chapter.

$M(1)O_4(OH)_2$ and its three-dimensional framework

According to the results of chemical analyses, structure refinement, bond valence calculation and mean M(1)-(O,OH) distances, Fe^{3+} and $(Fe,Zn)^{2+}$ are randomly distributed in about equal amounts over the site M(1) (Tables 5 and 6). As already described, an attempt to prove the ordering of the di- and tri-valent cations, like in the ellenbergerite structure, was without success. Structure determination and refinement in the possible subgroup $P6_3$

Table 4. Atomic coordinates and displacement parameters ($x10^{-4}$) of ekatite.

Atom	Wyck.	Occup.	x	y	z	U11	U22	U33	U23	U13	U12	U_{eq}
Fe(1)	12d	0.508	0.91549(8)	0.57285(9)	0.5935(2)	127(4)	98(4)	101(5)	8(4)	–2(4)	59(3)	107(3)
Fe(2)	12d	0.337	0.91549(8)	0.57285(9)	0.5935(2)	127(4)	98(4)	101(5)	8(4)	–2(4)	59(3)	107(3)
Zn(2)	12d	0.150	0.91549(8)	0.57285(9)	0.5935(2)	127(4)	98(4)	101(5)	8(4)	–2(4)	59(3)	107(3)
As(1)	6c	0.50	0.71631(8)	0.85816(4)	0.6246(3)	75(4)	70(3)	85(5)	–2(2)	–5(4)	38(2)	77(3)
As(2)	2b	0.128	0.66667	0.33333	0.895(1)	74(11)	74(11)	64(31)	0	0	37(6)	71(14)
Si(2)	2b	0.041	0.66667	0.33333	0.837(1)	76	76	202	0	0	38	77
O(1)	6c	0.5	0.6048(8)	0.8024(4)	0.886 (2)	164(43)	252(39)	109(40)	27(15)	54(30)	82(21)	185(26)
O(2)	12d	1.0	0.6559(6)	0.9339(5)	0.437(1)	187(29)	76(24)	127(25)	–11(18)	–61(20)	76(21)	125(15)
O(3)	6c	0.5	0.5968(4)	0.1936(8)	0.723 (2)	215(38)	43(35)	334(52)	–70(33)	–35(16)	21(18)	216(26)
OH(4)	6c	0.5	0.0490(7)	0.5245(3)	0.778(2)	104(33)	117(26)	163(37)	20(13)	40(27)	52(17)	129(19)
OH(5)	2b	0.041$^{1)}$	0.66667	0.33333	0.166(4)							94(53)
H(1)	6c	0.5$^{2)}$	0.01(1)	0.502(6)	0.60 (3)							
H(2)	2b	0.041$^{1)}$	0.66667	0.33333	0.38810$^{2)}$							

The anisotropic displacement factor exponent is defined as: $-2\pi^2[h^2a^{*2}U_{11} + ... + 2hka^*b^*U_{12}]$.
$^{1)}$: fixed according to the Si content; $^{2)}$: fixed

Table 5. Selected atomic distances (Å) and angles (°) for ekatite.

M(1) – O(2)	1.984(5)	As(1) – O(2)	1.783(3) x2
M(1) – O(1)	1.985(5)	As(1) – O(1)	1.807(3)
M(1) – O(3)	2.012(5)	mean	1.791
M(1) – O(2)'	2.072(5)		
M(1) – OH(4)	2.202(6)	As(2) – O(3)	1.773(9) x3
M(1) – OH(4)	2.284(6)		
mean	2.090	Si(2) – O(3)	1.65(2) x3
		Si(2) – OH5	1.66(19)
H(1) – OH(4)	1.01	mean	1.65
H(1) – OH(4)'	1.75		
H(2) – OH(5)	1.12		
H(2) – O(3)	2.29		
O(1) – M(1) – O(2)	104.8(3)	O(1) – As(1) – O(1)'	98.7(4)
O(1) – M(1) – O(2)'	92.6(3)	O(1) – As(1) – O(2)	97.7(3)
O(1) – M(1) – O(3)	102.5(3)		
O(1) – M(1) – OH(4)	96.4(3)	O(3) – As(2) – O(3)'	98.1(5)
O(1) – M(1) – OH(4)'	171.9(3)	O(3) – As (2) – OH5	119.3(4)
O(2) – M(1) – O(2)'	92.0(2)		
O(2) – M(1) – O(3)	97.1(3)	O(3) – Si(2) – O(3)'	108.6
O(2) – M(1) – OH(4)	158.5(3)	O(3) – Si(2) – OH5	110.3
O(2) – M(1) – OH(4)'	83.3(2)		
O(2)'– M(1) – O(3)	160.0(3)		
O(2)'– M(1) – OH(4)	83.4(2)	OH(4) – H(1) – OH(4)'	170.3
O(2)'– M(1) – OH(4)'	85.9(2)	OH(5)5 – H(2) – O(3)	137.6 x3
O(3) – M(1) – OH(4)	81.6(3)		
O(3) – M(1) – OH(4)'	77.5(3)		
OH(4) – M(1)– OH(4)'	75.6(1)		

M(1) = 0.5 Fe^{3+} + 0.42 Fe^{2+} + 0.08 Zn, derived from the chemical composition

Table 6. Bond valence table for ekatite.

	0.5Fe^{3+}	*0.42Fe*$^{2+}$	*0.08Zn =*	$\Sigma M^{2.5+}$	$As^{3-}(1)$	*0.7As(2)*	*0.3Si(2)*	$\Sigma X^{3.3-}(2)$	ΣO
O(1)	*0.27*	*0.21*	*0.04*	0.52 2x→	0.96	–.–	–.–	–.–	2.00
O(2)	*0.27* *0.21*	*0.21* *0.17*	*0.04* *0.03*	0.52 0.41	1.02 2x↓	–.–	–.–	–.–	1.95
O(3)	*0.25*	*0.20*	*0.04*	0.49 2x→	–.–	*0.73*	*0.28*	1.01 3x↓	1.99
OH(4)	*0.15* *0.12*	*0.12* *0.10*	*0.02* *0.02*	0.29 2x→ 0.24 2x↓	–.–	–.–	–.–	–.–	1.06
OH(5)	–.–	–.–	–.–	–.–	–.–	–.–	*0.30* 0.90→	0.30↓	0.90
Σ M,X				2.47	3.00			3.33	

The partial values of the cations are given in *italics*: M = Fe^{3+}, Fe^{2+} and Zn^{2+} at the second and X(2) = As^{3+} and Si^{4+} at the third column, respectively.

give neither better R-values nor significantly different mean $M(1)^{3+}$-(O,OH) and $M(1)^{2+}$-(O,OH) distances 2.079 and 2.097 Å, respectively. Therefore, it is assumed that Fe^{3+}, Fe^{2+} and Zn are randomly distributed over the octahedral site hence the space group $P6_3mc$. Should sufficient natural or synthetic material be available in the future, this can be proved easily by spectroscopic investigation (*e.g.* Mössbauer).

M(1) is situated in general position and forms strongly distorted $M(1)O_4(OH)_2$ octahedra that build up $M(1)_2O_7(OH)_2$ dimers by common OH(4)-O(3)-OH(4) faces (Fig. 2, 4). The remarkable bond-lengths variation, M(1)-O 1.984(5) to 2.072(5) Å and M(1)-OH 2.202(6) and 2.284(6) Å (Table 5 and Fig. 4), can be interpreted in terms of the distinct anion bond-valence requirements of O^{2-} or OH^- (Table 6). Cation-cation repulsion due to the short M(1)-M(1) distance, $Fe^{(3+,2+)}$-$Fe^{(3+,2+)}$ = 2.940 Å, may have supported the arrangement of two OH at the shared octahedral face (Fig. 4).

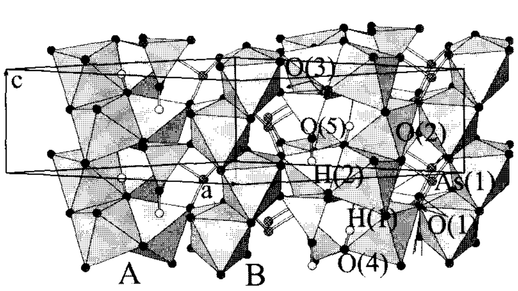

Fig. 3. Crystal structure of ekatite seen along [001]. A and B indicate a perpendicular and clinographic view, respectively, on the zigzag double chains of octahedral dimers. The O(5) vertices of the $HO(5)Si(2)O(3)_3$ tetrahedra all point into the same direction.

The dimeric octahedral units form zigzag double chains extending along [001] by O(2)-OH(4) edges like a ribbon of the NiAs structure type parallel [110] (Fig. 3). Finally, such double chains link together by O(1) vertices to give a three-dimensional $(M(1)_{12}(OH)_6O_{24})^{24-}$ framework of densely packed trigonal rods with small triangular and large hexagonal channels along the three-fold and the 6_3 screw axes, respectively (Fig. 2 and 5a).

AsO_3 groups, substitution by $HOSiO_3$

Both the AsO_3 groups form unpolymerized trigonal pyramids with stereoactive lone-pair electrons on each As^{3+} atom. While the trigonal pyramids of As(2) display ideal $3m$ site symmetry, those of As(1) is slightly distorted. In accordance with its point symmetry m, the $As(1)O_3$ group has a longer bond on the mirror plane, As(1)-O(1) 1.807(3) Å, and two shorter bonds, As(1)-O(2) 1.783(3) Å (Fig. 4). Whereas the first oxygen is the common corner of two trigonal rods, each of the latter belongs to two different zigzag double chains (Fig. 2 and 3). The As-O distances and angles (Table 5) fit well with data given in the literature (ICSD, 2000).

$As(1)O_3$ groups are located along the walls of the large hexagonal channels and the lone-pair electrons of As(1) are directed toward the channel centre. It is noteworthy that As(1) occupies the position of face-sharing trigonal antiprism, with an empty centre (Fig. 5a). Its dimensions are As(1)-

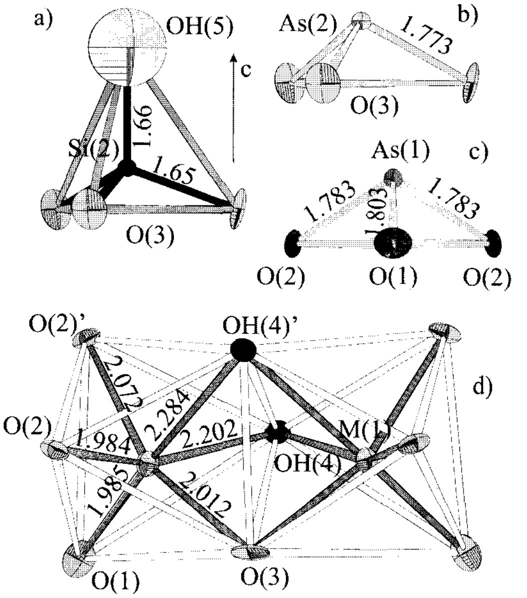

Fig. 4. ORTEP drawings of some coordination polyhedra of ekatite: (a) $HOSi(2)O_3$ and (b) $As(2)O_3$, both parallel to the *c*-axis; (c) $As(1)O_3$, and the strongly deformed $M(1)_2O_7(OH)_2$ dimer (d), viewed along the *c*-axis. Whereas OH(5) displays an unusually large isotropic displacement parameter, all others show usual values of anisotropy.

As(1) 4.028 and 5.435 Å and As(1)-□ 3.201 and 3.666 Å, respectively.

The $As(2)O_3$ pyramids are situated on the three-fold axes in the centre of the small trigonal channel. Its As and their lone-pair electrons point all in the same direction (Fig. 2) and cause the polarity of the structure, proved by an ideal Flack parameter (Table 3). As a peculiarity, $HOSi(2)O_3$ with point symmetry $3m$ replaces about one third of the $As(2)O_3$, in random distribution. The OH apex points in the same direction as the lone-pair electrons of the $As(2)O_3$ group. However, due to the large isotropic displacement factor of OH (Fig. 4) and the uncertain result of anisotropic refinement, its position on the three-fold axis may not be ideally realized, but deviations along the x- and y-axis may occur. The Si-O and Si-OH bond distances fit well with mean literature values and with the bond-valence calculations (Table 6).

Hydrogen bonds

The site of H(1) is evidently proved by structure determination and the resulting bond distances (Table 5) as well as by the result of empirical bond-valence calculations (Table 6). H(1) belongs with its short bond, H(1)-O(4) 1.01 Å, to the OH(4) (Fig. 3) like in other structurally related minerals and compounds (see below). There is only one possible acceptor distance with H(1)-OH(4) 1.75 Å to another OH(4). H(2) is part of OH(5) (Fig. 3), but the exact position of H(2) and its hydrogen bonds are rather uncertain. Due to the large isotropic displacement factor of OH(5) (Fig. 4, Table 4), both atoms might be distributed randomly around the three-fold axis (for H(2) to a larger extent). However, refinements on 6c positions instead of 2b end with worse results.

Bond-valence calculation

Bond-valence calculation using the empirical values of Brese & O'Keeffe (1991) gave further evidence for several topics discussed above (Table 6), espe-

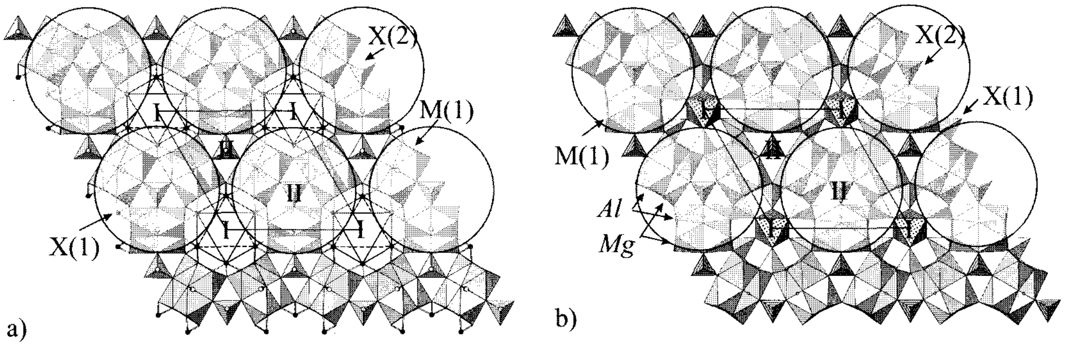

Fig. 5. Structural relationships between the ekatite (a) and phosphoellenbergerite (b) structure types. The trigonal rods are circled. I and II indicate the hexagonal and triangular channels, respectively. (a). In the hexagonal channel I, the edges of the empty trigonal prisms with As(1) at their corners are delineated. $As(2)O_3$ and $HOSi(2)O_3$ are randomly distributed in channel II. (b) The hexagonal channel is completely filled with face-sharing M(2) octahedra. The Al-Mg ordering scheme of M(1) in the structure of ellenbergerite is indicated by *italics*.

cially for the existence of OH(4) (Σ 1.06 v.u.) and OH(5) (Σ 0.90 v.u.). The distribution of di- and trivalent cations on site M(1) fits also very well with the theoretical and calculated values 2.50 and 2.47, respectively, as well as with the charge sum of O(1) to O(3), within the usual uncertainties. The replacement of about 1/3 As^{3+} by Si^{4+} on the site of As(2) produces excellent values ΣX(2) 3.33 v.u. and ΣO(3) 1.99 v.u.. No additional arguments, however, could by given for the hydrogen-bond system.

Structural relationships

Typical for all crystal structures related with ekatite are densely packed zigzag double chains formed by $M(1)O_4(OH)_2$ octahedra dimers, as already described for ekatite (Fig. 3). They are the bones of a three-dimensional skeleton with two types of parallel channels. The small triangular channel in the centre of three corner-sharing double chains is always occupied by complex anions. The result are trigonal rods (Fig. 5 and 6), which are a common feature of all related structure types discussed above. Distinctive differences are developed with respect to the large hexagonal channels, either by the occurrence of coordination polyhedra – different in size and/or degree of occupancy – or the existence or non-existence of such channels (Fig. 5 and 6).

Ekatite, with the general formula $M(1)_{12}X(2)_2X(1)_6(OH)_6(O,OH,\square)_{26}$ represents an open structure type, only with $X(1)O_3$ in the hexagonal channel (Fig. 5a). It is also adopted by hydroxyphosphites, $P6_3mc$, $(M(1)_{11}\square)(OH)_6(HPO_3)_8$, of Co, Ni and Zn (Marcos *et al.*, 1993a and b), as well as of Mn and Fe (Attfield *et al.*, 1994). The rather small differences are: (i) $HX(1)O_3$ instead of $X(1)O_3$, and (ii) one empty M(1) site in random distribution, according to stoichiometry. These compounds became of interest as a new family of microporous materials that involve infinite channels with window sizes up to about 4 Å. Of the same interest are synthetic hydroxytellurites (Perez *et al.*, 1976) and hydroxyselenites (Amorós *et al.*, 1996) of Ni^{2+} and Co^{2+}, with the general formula $M(1)_{12}(OH)_6[X(1)O_3]_2[X(2)O_3]_6(OH)_2$ and space group $P6_3mc$. They are structurally very close to ekatite, but with additional $(OH)_2$ in the hexagonal channel.

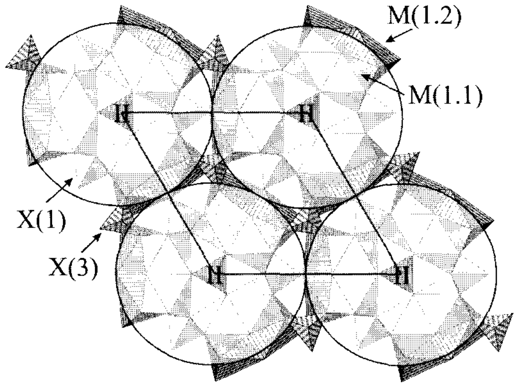

Fig. 6. The crystal structure of holtedahlite: a dense packing of II-rods known from the ekatite and the phosphoellenbergerite structures. The ordering of M(1) cations of holtedahlite is given as M(1.1) and M(1.2). Note that only one half of the X(1) polyhedra of ekatite occurs in holtedahlite, the other half is replaced by X(3) in different orientation.

The structural relationships between ekatite and holtedahlite, $Mg(1)_6Mg(2)_6(OH,O)_6[HOP(1)O_3, CO_3][P(2)O_4]_2[P(3)O_4]_3$, $P31m$ (Rømming & Raade, 1989), is mainly characterized by loss of the large hexagonal channels, so typical for the ekatite and phosphoellenbergerite structure types. The triangular rods (II) of the structures discussed so far are densely packed repeating-units in holtedahlite (Fig. 6). The zigzag double chains consist of face-sharing Mg(1.1) octahedra dimers and Mg(1.2) octahedra dimers alternating along the *c*-axes. In the sheet of Mg(1.1) octahedra the double chains are connected by vertices of X(2) anions, $HOP(1)O_3$ and CO_3 in random distribution, and three X(1) anions $P(3)O_4$, which is one half of the complex X(1) anions of ekatite. Common vertices and two X(3) tetrahedra $P(2)O_4$, not known from the ekatite structure type, are the linking elements in the sheet of Mg(1.2) octahedra.

The structure type with the most densely packed hexagonal channels is represented by synthetic $Zn_{14}(OH)_6(SO_4)_2(VO_4)_6$ (Kato *et al.*, 1998) and phosphoellenbergerite, $[Mg,Fe,\square]_2Mg_{12}(OH)_6(HOPO_3,CO_3)_2(PO_4,HOPO_3,AsO_4)_6$ (Brunet & Schaller, 1996; Raade *et al.*, 1998), with space group $P6_3mc$ and general formula $M(2)_2M(1)_{12}X(2)_2X(1)_6(OH)_6(O,OH,\square)_{32}$ (Fig. 5b). Their hexagonal channel is filled by the coordination polyhedra of M(2) and X(1). Ellenbergerite, $[Mg,(Ti,Zr),\square]_2Mg_6(Al,Mg)_6(Si,P)_8O_{28}(OH)_{10}$, (Chopin *et al.* 1986; Comodi & Zanazzi, 1993) belongs to the same formula type. However, the M(1) cations of the face-sharing octahedra are ordered with one Mg and one Al in each dimer (Fig. 5b). The consequence is a change in symmetry from space group $P6_3mc$ to $P6_3$.

The structure comparison of ellenbergerite with magnesiodumortierite, idealized as $(Mg,Ti,\square)(Al,\square)_4(Al,Mg,\square)_2(OH)_3(BO_3)[(Si,\square)O_4]_3$, is fully described by Ferraris *et al.* (1995). Both structures are built up by two slabs. One type is common to both structures, but the second differs to such an extent that a transformation of dumortierite minerals into an ellenbergerite-type hexagonal polymorph, as suggested by Moore & Araki (1978), would be far from straightforward (Ferraris *et al.*, 1995). Therefore, the term "dumortierite family" should not be used for the synthetic compounds as introduced by Marcos *et al.* (1993a and b), but ekatite or phosphoellenbergerite are appropriate.

There are obvious relations between the conditions of formation and features of the structure types. Ekatite, with its large empty hexagonal channels, and the structurally related chemical compounds have been formed from aqueous solutions at low temperature and, if at all, low pressure. The cations are mainly transition-metals. The densely packed phosphoellenbergerite structure type, however, represents mainly Mg-Al minerals, which originate from high- to ultra-high-pressure metamorphic rocks.

Acknowledgements: I am very grateful to all colleagues who have supported the description of the new mineral with important contributions, especially Prof. Dr. Th. Schleid and Dr. F. Lissner, Stuttgart. X-ray data were collected and the IR-spectra performed by Dr. F. Lissner and M. Häußlein, respectively, Institut für Anorganische Chemie, Universität Stuttgart. Drs. F. Fontan and Ph. de Parseval, Université Paul Sabatier, Toulouse, have verified the microprobe data. Mrs Sumati Panicker-Otto has improved the English text. The manuscript has also benefited from the comments of the referees Paola Comodi and Gunnar Raade.

References

Amorós, P., Marcos, M.D., Roca, M., Beltrán-Porter, A., Beltrán-Porter, D. (1996): Synthetic pathway for new tubular transition-metal hydroxo- and fluoro-selenites: crystal structure of $M_{12}(X)_2(SeO_3)_8(OH)_6$ ($M = Co^{2+}$, Ni^{2+}; $X = OH^-$). *J. Solid State Chem.*, **126,** 169-176.

Attfield, M.P., Morris, R.E., Cheetham, A.K. (1994): Synthesis and structures of two isostructural phosphites, $Fe_{11}(HPO_3)_8(OH)_6$ and $Mn_{11}(HPO_3)_8(OH)_6$. *Acta crystallogr.*, **C50**, 981-984.

Brese, N.E. & O'Keeffe, M. (1991): Bond-valence parameters for solids. *Acta crystallogr.*, **B41**, 192-197.

Brunet, F. & Schaller, T. (1996): Protons in the magnesium phosphates phosphoellenbergerite and holtedahlite: an IR and NMR study. *Amer. Mineral.*, **81**, 385-394.

Chopin, C., Klaska, R., Medenbach, O., Dron, D. (1986): Ellenbergerite, a new high-pressure Mg-Al-(Ti,Zr)-silicate with a novel structure based on face-sharing octahedra. *Contrib. Mineral. Petrol.*, **92**, 316-321.

Comodi, P. & Zanazzi, P. F. (1993): Structural study of ellenbergerite. Part I: Effects of high temperature. *Eur. J. Mineral.*, **5**, 819-829.

Ferraris, G., Ivaldi, G., Chopin, C. (1995): Magnesiodumortierite, a new mineral from very-high-pressure rocks (Western Alps). Part I: Crystal structure. *Eur. J. Mineral.*, **7**, 167-174.

Gebhard, G. (1991): Tsumeb, eine deutsch-afrikanische Geschichte. C. Gebhard, Gießen, 239 p.

Herrendorf, W. (1997): Programm HABITUS, Gießen, 1995; Fa. STOE & Cie GmbH: Programm X-SHAPE, Version 1.02, Darmstadt, 1997.

ICSD (2000): Release 2000/1. Fachinformationszentrum Karlsruhe and National Institute of Standards and Technology Gaithersburg.

Kato, K., Kanke, Y., Oka, Y., Yao, T. (1998): Crystal structure of zinc hydroxide sulfate vanadate(V), $Zn_7(OH)_3(SO_4)(VO_4)_3$. *Z. Kristallogr. – New Cryst. Struc.*, **213**, 26.

Keller, P. (1984): Tsumeb/Namibia – eine der spektakulärsten Mineralfundstellen der Erde. *Lapis*, **9**, H. 7&8, 13-62.

Keller, P. & Innes, J. (1986): Neue Minerale von Tsumeb. *Lapis*, **11**, H. 9, 28-32.

Keller, P., Lissner, F., Schleid, Th. (1999): $(Fe^{3+},Fe^{2+})_6(OH,O)_3[AsO_3]_3[AsO_3, HOSiO_3]$: Ekatit, ein hydrogensilicathaltiges Eisen(III/II)-Hydroxid-Oxoarsenat(III). *Z. Kristallogr., Supl.* **16**, 84.

Mandarino, J.A. (1981): The Gladstone-Dale relationship: Part IV. The compatibility concept and its application. *Canad. Mineral.*, **19**, 441-450.

Marcos, M.D., Amorós, P., Le Bail, A. (1993a): Synthesis and crystal structure of tubular hydroxyphosphite: $Zn_{11}\square(HPO_3)_8(OH)_6$. *J. Solid State Chem.*, **107**, 250-257.

Marcos, M.D., Amorós, P., Beltrán-Porter, A., Martíñes, R., Attfield, P. (1993b): Novel crystalline microporous transition-metal phosphites $M_{11}(HPO_3)_8(OH)_6$ (M = Zn, Co, Ni). X-ray powder diffraction structure determination of the Co and Ni derivates. *Chem. Mater.*, **5**, 121-128.

Moore, P.B. & Araki T. (1978): Dumortierite, $Si_3B[Al_{6.75}\square_{0.25}O_{17.25}(OH)_{0.75}]$: a detailed structure analysis. *N. Jb. Mineral. Abh.*, **132**, 231-241.

Perez, G., Lasserre, F., Moret, J., Maurin, M. (1976): Structure cristalline des hydroxytellurites de nickel et de cobalt. *J. Solid State Chem.*, **17**, 143-149.

Raade, G., Rømming, C., Medenbach, O. (1998): Carbonat-substituted phosphoellenbergerite from Modum, Norway: description and crystal structure. *Mineral. Petrol.*, **62**, 89-101.

Rømming, C. & Raade, G. (1989) The crystal structure of natural and synthetic holtedahlite. *Mineral. Petrol.*, **40**, 91-100.

SHELXTL (1996): Version 5, Siemens Analytical Instruments Inc., Madison, Wi.

SHELXL-97 (1997): G. M. Sheldrick, Univ. Göttingen, Copyright © George M. Sheldrick, 1993-7.

Received 26 September 2000
Modified version received 6 February 2001
Accepted 14 February 2001